Proc. NIPR Symp. Polar Meteorol. Glaciol., **9**, 23–32, 1995

BUBBLE FORMATION EXPERIMENTS IN SNOW DENSIFICATION

Seigo ISHII[1], Hideki NARITA[2] and Norikazu MAENO[2]

[1]*INA Corporation, 44–10, Sekiguchi 1-chome, Bunkyo-ku, Tokyo 112*
[2]*Institute of Low Temperature Science, Hokkaido University, Kita-19, Nishi-8, Kita-ku, Sapporo 060*

Abstract: Bubble formation experiments were conducted for snow composed of ice spheres 303 μm in diameter at various temperatures and applied pressures. By measuring volumes of closed-off bubbles at various densities, the bubble formation density (ρ_f) and the bubble close-off density (ρ_c) were obtained. ρ_f, that is the density at which bubble formation begins, decreased with lowering temperature or pressure. On the other hand, ρ_c, that is the density at which bubble formation finishes, increased with lowering temperature or pressure.

1. Introduction

In the densification process of snow in polar regions, air voids, which are initially connected to the atmosphere, are disconnected and some fraction is closed off in ice at a depth interval typically 40 to 120 m from the surface. The amount, chemical composition and other properties of air trapped in bubbles (hereafter air voids completely closed off in ice are specified as bubbles in this paper) give important information on past ice sheets and climates, especially the total gas content measured from deep drilled ice cores, which in turn gives the past temperature and elevation of ice sheets (RAYNAUD and LORIUS, 1973; RAYNAUD and LEBEL, 1979). However, according to recent work by MARTINERIE *et al.* (1992), the relation between the total gas content and temperature is not simple but depends on temperature and possibly on wind.

On the other hand, SCHWANDER and STAUFFER (1984) pointed out that the depth distribution of the bubble close-off process gives a large difference in the age of ice and the trapped air. The difference may amount to 100 to 3000 years, depending on the temperature and accumulation rate. It is clear that the age difference might cause serious errors in interpreting obtained results of past climatic variations.

One of the most promising ways to settle the above questions is to understand properly the bubble formation mechanism in snow densification. This paper reports results of bubble formation measurements in snow densification carried out under known physical conditions including temperature, applied pressure and ice particle diameter.

2. Experimental Procedures

Densification experiments were conducted by uniaxially compressing a snow sample packed in a stainless steel cylindrical container. The sample was an aggregate of ice spheres formed by freezing sprayed water droplets in liquid nitrogen and sieved to have

a mean diameter of 303 ± 60 μm. The container was a thick tube of inner diameter 20 mm and height 100 mm, to which two stainless steel compression pistons of the same diameter were connected vertically. The densification was performed by applying constant loads, 0.5, 1.0 or 2.0 MPa. The displacement of the upper piston was measured by a linear strain-gauge and recorded in a microcomputer, from which the bulk density of the sample was calculated assuming that the mass of the sample does not change during the experiment. The mass was measured before and after each run. More details of the experimental procedure are found in EBINUMA and MAENO (1985).

Each experiment was carried out by placing five similar sample sets in a large thermally insulated box, the temperature of which was kept at -5, -10 or -20°C to an accuracy of ± 0.1°C. In each experimental run at constant pressure and temperature the samples were taken out to measure the volume of bubbles isolated in ice and for microphysical observation of thin sections.

The volume of isolated bubbles in a snow sample was measured using a method similar to that developed by STAUFFER *et al.* (1985). Our measuring device was composed of three stainless steel vessels, 38, 45 and 72×10^{-6} m^3 in volume, each of which can be connected or disconnected to the atmosphere, other vessels or pressure gauge through pipes. When one of the vessels containing a sample, typically 10^{-5} m^3 in volume, is disconnected from the atmosphere and connected to a previously evacuated vessel, the air inside expands. If the expansion proceeds slowly and isothermally the volume of bubbles isolated in ice can be estimated from the measured pressure drop assuming the ideal gas law. The measurement is essentially that of volume of air voids which are not trapped in the ice matrix, so that the obtained volume of bubbles is that existing in the ice matrix and may be over-estimated because of general higher pressures produced at sample edges during densification. Then the specimens for the bubble volume measurements were prepared from internal parts of samples. The effect of water vapor on the measured bubble volume was estimated to be only a few percent and was not taken into account in the present analyses.

3. Snow Densification Mechanisms during Bubble Formation

Figure 1 shows typical time variations of bulk density at different temperatures (-5, -10 and -20°C) and applied pressures (0.5, 1.0 and 2.0 MPa). The increase in the densification rate when the temperature or pressure is increased is apparent. According to MAENO and EBINUMA (1983), dry snow densification proceeds through four distinct stages (I-IV). The three critical densities dividing stages I / II, II / III, and III / IV are roughly 550, 700 and 830 kg/m^3, which are considered to depend mainly on temperature and pressure. The density-time relations as shown in Fig. 1 were replotted on log $\dot{\varepsilon}$–ρ diagrams to determine the second II / III critical density, where $\dot{\varepsilon}$ is the strain rate of densification defined as $\dot{\varepsilon} = (\mathrm{d}\rho/\mathrm{dt})/\rho$ and ρ is the density. The II / III critical density was found as the point of slope change of the linear relation, corresponding to alteration of the densification mechanism. The II / III critical density increased with the rising temperature or decreasing pressure (Table 1) in agreement with the result of EBINUMA and MAENO (1985). They concluded that it is the density at which the dislocation creep mechanism becomes effective because of the sufficient contact area

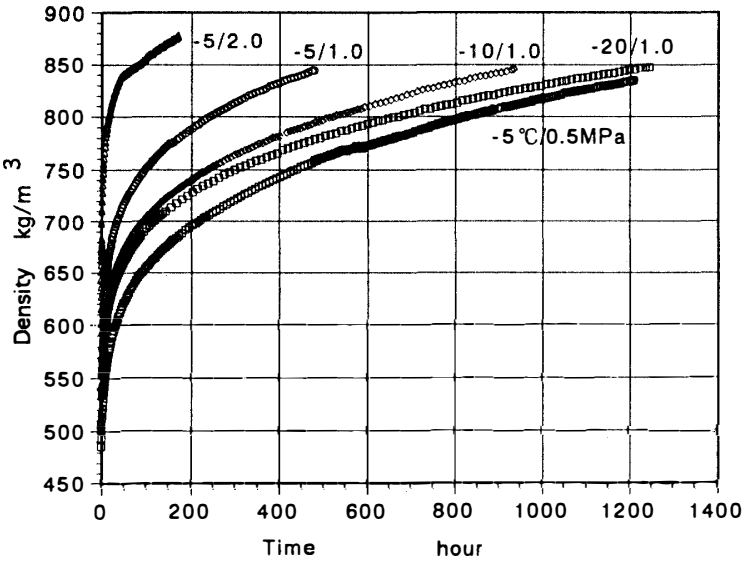

Fig. 1. Time variations of density at different temperatures, −5, −10 and −20°C, and pressures, 0.5, 1.0 and 2.0 MPa. Time intervals of data points plotted are roughly 0.5 to 2 hours.

Table 1. The II/III critical density at which the relation between the strain rate of densification and density changes. Unit in kg/m³.

	Pressure		
Temperature	0.5 MPa	1.0 MPa	2.0 MPa
−5°C	679	706	743
−10	—	700	—
−20	—	695	—

formed between individual particles (EBINUMA and MAENO, 1987).

Figure 2 gives the strain rate of densification in stages II and III plotted against applied pressure at −10°C, which shows that the relation can be expressed by the following power law equation:

$$\dot{\varepsilon} = A\sigma^n, \tag{1}$$

where σ is the applied stress, and A and n are constants. It is evident in the figure that the power index decreases from 5.1 to 1.8 as the density increases from 596 to 826 kg/m³. The result can be explained as follows. The densification below the critical II/III density around 700 kg/m³ proceeds by particle rearrangement expressed by a power law with n as large as 5; above the critical density, the contact between individual particles attains an optimum or maximum state and the densification through dislocation creep, typically $n \fallingdotseq 3$, becomes predominant. As the density approaches the III/IV critical density, or bubble close-off density, the power index decreases and approaches unity.

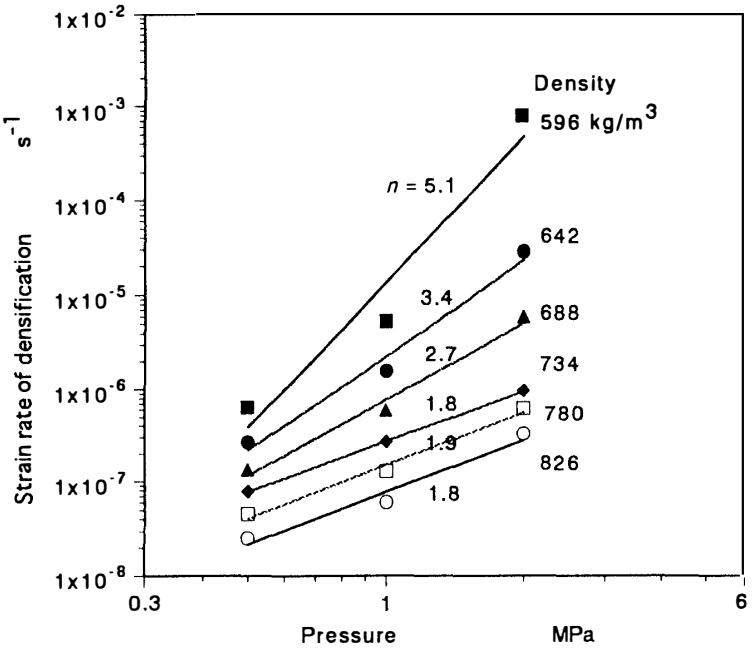

Fig. 2. Strain rate of densification versus applied pressure. The parameter is density, and n is the power index in eq. (1).

4. Volumes of Bubbles Formed in Snow Densification

Measured volumes of bubbles enclosed in ice are given in Fig. 3, in which the volumes are expressed in m^3 per 1 kg of ice. It is natural to assume that the volume is filled with air at the experimental temperature and air pressure. Each diagram in Fig. 3 shows that the formation of bubbles begins and ceases at some densities in the III stage of densification. We call the former the bubble formation density (ρ_f) and the latter the bubble close-off density (ρ_c), the two corresponding to the start and end of stage III. Each of the measured bubble volumes (V) can be fitted by the following equation when the density is smaller than ρ_c:

$$V = a(\rho/\rho_i)^b, \tag{2}$$

where a and b are constants and ρ_i is the density of ice (917 kg/m^3). The numerical values are listed in Table 2. The linear decrease in V after the close-off density is due to the shrinkage of bubbles by compression. The bubble close-off density was determined as the density where eq. (2) crosses a straight line in each diagram, and the bubble formation density was calculated from eq. (2) by putting $V = 3\times10^{-6}$ m^3/kg, which corresponds to the experimental error in our measurement. The bubble close-off density could not be observed in the experimental working time when the densification proceeded too slowly as in Fig. 3A; in such cases the density at the maximum measured bubble volume was regarded as the bubble close-off density. The obtained values of ρ_f and ρ_c are listed in Table 3.

Figure 4 gives the temperature (A) and pressure (B) dependences of the bubble

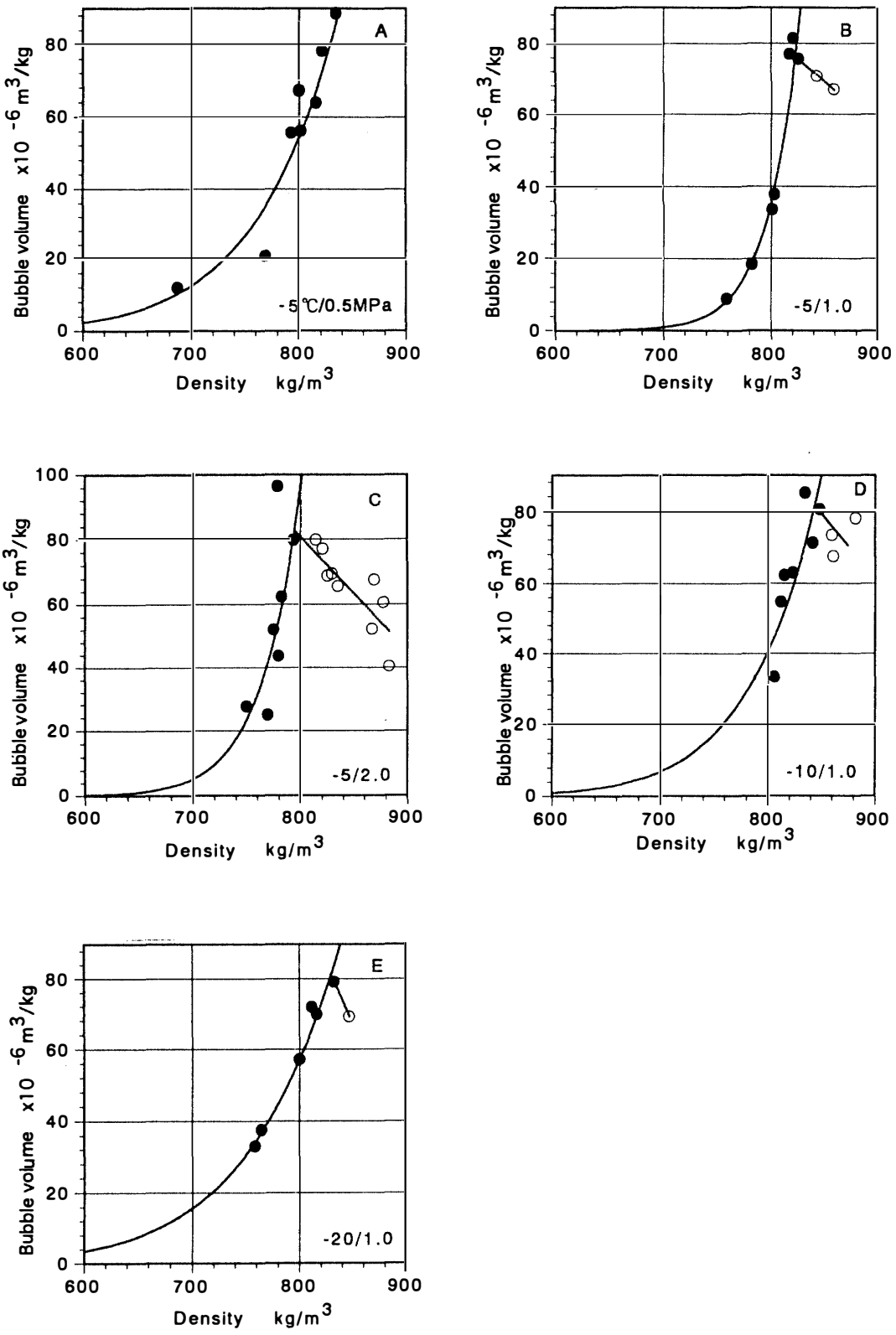

Fig. 3. Volumes of bubbles trapped in ice versus density.

Table 2. Numerical values eq. (2). Units: bubble volume in m^3/kg, density in kg/m^3 and a in m^3/kg.

	Pressure					
	0.5 MPa		1.0 MPa		2.0 MPa	
Temperature	*a*	*b*	*a*	*b*	*a*	*b*
− 5°C	1.42×10^{-4}	10.9	1.52×10^{-4}	27.6	1.25×10^{-3}	21.7
−10	—	—	2.16×10^{-4}	13.2	—	—
−20	—	—	2.05×10^{-4}	9.71	—	—

Table 3. Bubble-formation density (ρ_f) and close-off density (ρ_c). Unit in kg/m^3.

	ρ_f			ρ_c		
	Pressure			Pressure		
Temperature	0.5 MPa	1.0 MPa	2.0 MPa	0.5 MPa	1.0 MPa	2.0 MPa
− 5°C	613	731	694	>835	823	795
−10	—	662	—	—	849	—
−20	—	593	—	—	834	—

formation and close-off densities. The bubble formation density is shown to decrease with the lowering temperature or pressure, that is, the close-off of individual bubbles begins at smaller densities when the temperature or pressure is low. On the other hand, the bubble close-off density increases slightly with the lowering temperature or pressure, that is, the close-off of the last bubble takes place at larger densities when the temperature or pressure is low. The numerical relations are as follows:

$$\rho_f = 765.5+8.871\,\theta = -1656+8.871\,T \quad \text{at } 1.0\,\text{MPa}, \tag{3}$$

$$\rho_f = 41.0P+631.5 \quad \text{at } -5^\circ\text{C}, \tag{4}$$

$$\rho_c = 830.5\ -0.414\,\theta = 943.5\ -0.414\,T \quad \text{at } 1.0\,\text{MPa}, \tag{5}$$

and

$$\rho_c = -26.8P+849.0 \quad \text{at } -5^\circ\text{C}, \tag{6}$$

where θ, T and P are the temperature in °C and K, and the applied pressure in MPa, respectively.

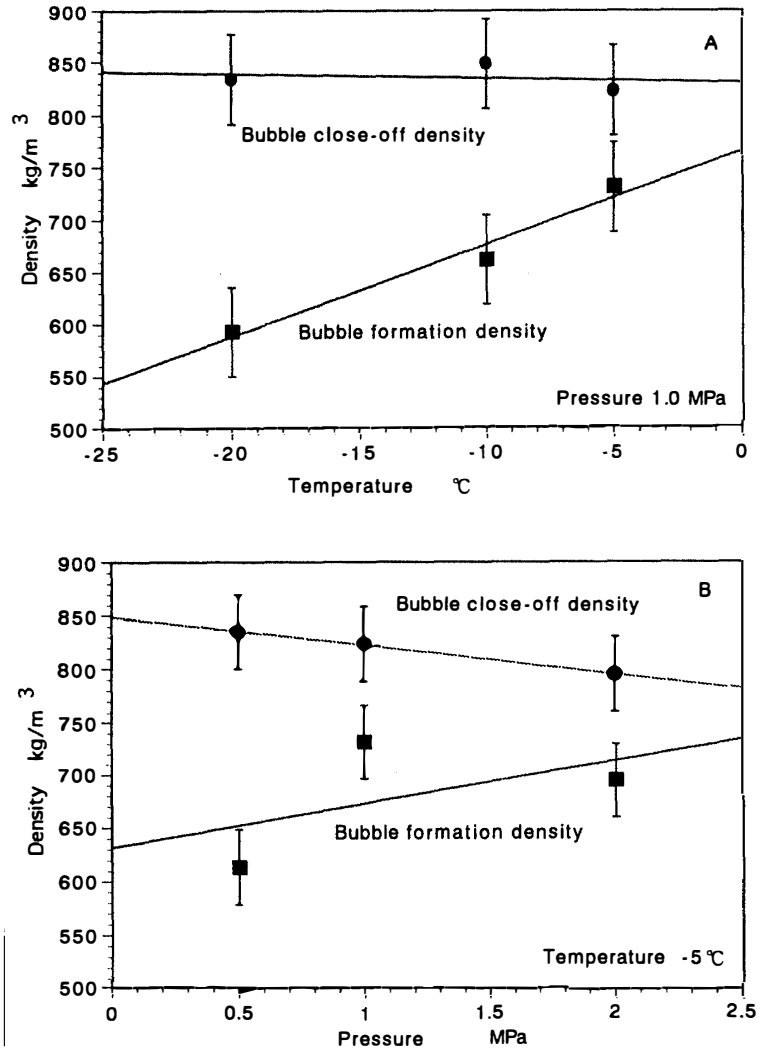

Fig. 4. Temperature (A) and pressure (B) dependences of bubble formation density and bubble close-off density.

5. Microscopic Observations of Thin Sections

Thin sections were prepared for each sample after the bubble volume measurement to observe the change of shapes and sizes of air voids during densification. The sample surface was first reinforced with aniline at $-15\,^{\circ}C$ and a smooth observation plane was cut in the middle part of the sample using a microtome. The plane surface, vertical to the compression direction, was then treated with rose-colored dye powder (eosin, insoluble in water and mean diameter 5 μm), and was minimum planed again with a microtome. Then cut bubbles on the surface appeared vividly due to embedded color dye, on which microscopic observations were made by using reflected light. The technique enabled us to measure sizes and shapes of bubbles cut by a geometrical plane; otherwise, *e.g.* with thin sections under transmitted light, it is quite difficult to distinguish between the cut surface and periphery inside ice of a bubble. For smaller density samples, the aniline was

colored with black dye.

Figure 5 gives the mean cross-sectional area of bubbles plotted against the density at various temperatures and pressures. It is obvious that the mean cross-sectional area decreases with density, implying that, although the number of closed-off bubbles increases, their mean size decreases because of shrinkage through pressure-sintering mechanisms and splitting of larger bubbles. At the same time, the shape of bubbles becomes simpler on average.

Figure 6 shows the mean sphericity of bubbles, defined as the periphery of a bubble divided by that of the equal-area circle. At each temperature and pressure the mean

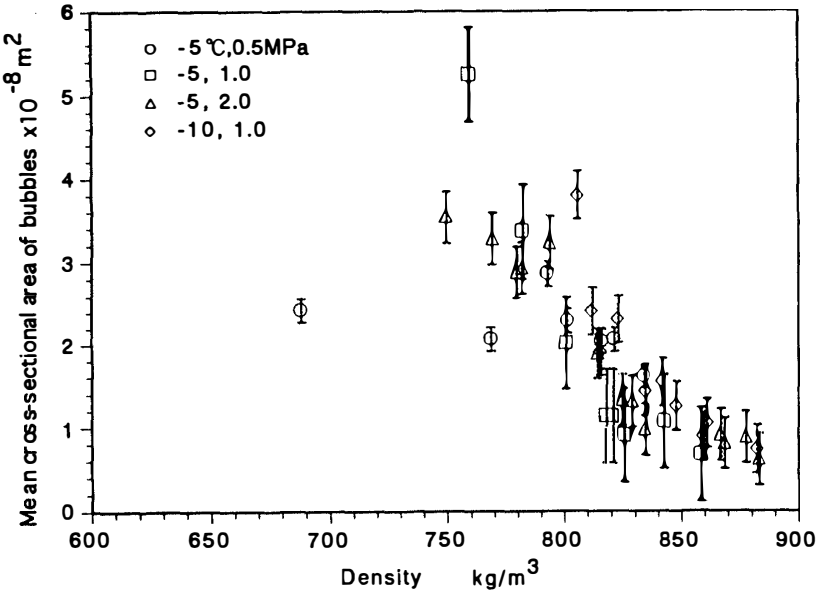

Fig. 5. Mean cross-sectional area of bubbles versus density.

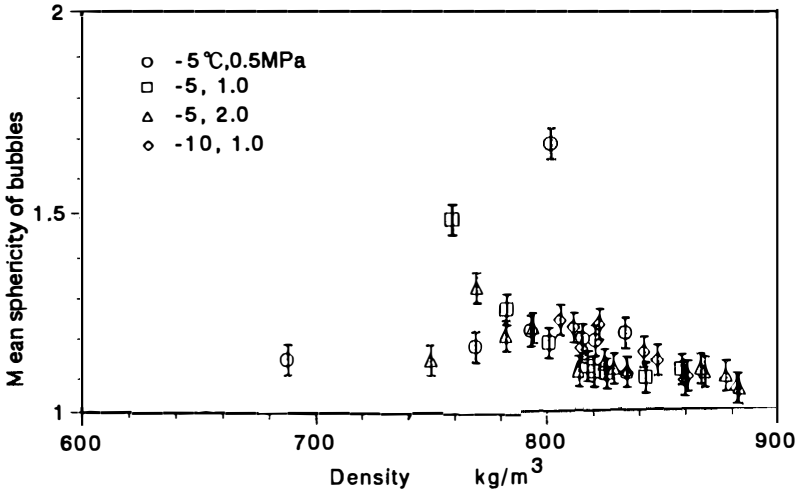

Fig. 6. Mean sphericity of bubbles versus density.

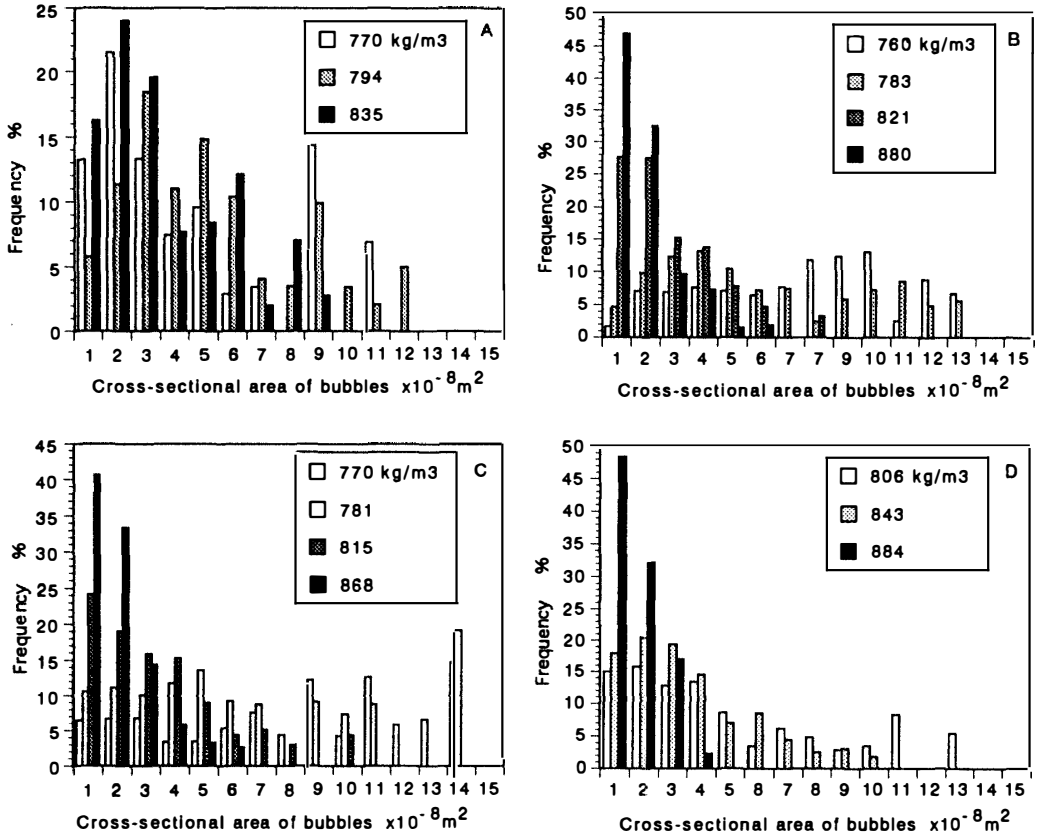

Fig. 7. Histograms of cross-sectional areas of bubbles. Temperatures and applied pressures in A, B, C and D are −5 °C/0.5 MPa, −5 °C/1.0 MPa, −5 °C/2.0 MPa and −10 °C/1.0 MPa respectively.

sphericity of bubbles decreases with density and approaches unity, that is spheres.

In Fig. 7, the distributions of cross-sectional areas of individual bubbles are shown to give more details of the geometrical structures. Each figure in Fig. 7 suggests that the number of larger bubbles decreases and that of smaller bubbles increases as the densification proceeds.

6. Concluding Remarks

The bubble formation experiment presented above confirmed that the bubble formation, that is the close-off of air voids in ice, takes place in stage III of snow densification and that the densities of initiation and termination of bubble formation depend strongly on applied pressure and weakly on temperature. The obtained results can be used to give important information to interpret and overcome the difficulties encountered in bubble studies of deep ice cores.

Acknowledgments

This work was carried out as a Master's Thesis of one of the authors (S.I.) at

Hokkaido University. The authors would like to express their thanks to M. ARAKAWA, M. HIGA, N. SUGI and H. TAKANO for their help in carrying out the work. The work was supported in part by a Grant-in-Aid for Scientific Research of Japanese Ministry of Education, Science and Culture.

References

EBINUMA, T. and MAENO, N. (1985): Experimental studies on densification and pressure-sintering of ice. Ann. Glaciol., **6**, 83–86.

EBINUMA, T. and MAENO, N. (1987): Particle rearrangement and dislocation creep in a snow-densification process. J. Phys., **48(C1)**, 263–269.

MAENO, N. and EBINUMA, T. (1983): Pressure sintering of ice and its implication to the densification of snow at polar glaciers and ice sheets. J. Phys. Chem., **87**, 4103–4110.

MARTINERIE, P., RAYNAUD, D., ETHERIDGE, D.M., BARNOLA, J.-M. and MAZAUDIER, D. (1992): Physical and climatic parameters which influence the air content in polar ice. Earth Planet. Sci. Lett., **112**, 1–13.

RAYNAUD, D. and LEBEL, B. (1979): Total gas content and surface elevation of polar ice sheets. Nature, **281**, 289–291.

RAYNAUD, D. and LORIUS, C. (1973): Climatic implications of total gas content in ice at Camp Century. Nature, **243**, 283–284.

SCHWANDER, J. and STAUFFER, B. (1984): Age difference between polar ice and the air trapped in its bubbles. Nature, **311**, 45–47.

STAUFFER, B., SCHWANDER, J. and OESCHGER, H. (1985): Enclosure of air during metamorphosis of dry firn to ice. Ann. Glaciol., **6**, 108–112.

(Receied November 14, 1994; Revised manuscript received February 1, 1995)